Developmental and Comparative Immunology 98 (2019) 80–88

Contents lists available at ScienceDirect

Developmental and Comparative Immunology

journal homepage: www.elsevier.com/locate/devcompimm

Genetic diversity of chemokine XCL1 and its receptor XCR1 in murine rodents

Feifei Xu[a,b,1], Dan He[a,b,1], Ruihong Ning[a,b], Bo Zeng[a,b], Cody W. Thompson[c], Ying Li[a,b], Dawei Wang[d], Yan Li[a,b,*]

[a] College of Animal Science and Technology, Sichuan Agricultural University, Wenjiang, People's Republic of China
[b] Farm Animal Genetic Resources Exploration and Innovation Key Laboratory of Sichuan Province, Sichuan Agricultural University, Wenjiang, People's Republic of China
[c] Department of Ecology and Evolutionary Biology and Museum of Zoology, University of Michigan, Ann Arbor, USA
[d] State Key Laboratory for Biology of Plant Diseases and Insect Pests, Institute of Plant Protection, Chinese Academy of Agricultural Sciences, Beijing, People's Republic of China

ARTICLE INFO

Keywords:
Genetic diversity
XCL1
XCR1
Murinae

ABSTRACT

The chemokine ligand XCL1 plays critical roles in immune responses with diverse physiological and pathological implications through interactions with a cognate G protein-coupled receptor XCR1. To shed insight into their versatile nature, we analyzed genetic variations of XCL1 and XCR1 in murine rodents, including commonly-used model organisms *Mus musculus* (house mouse) and *Rattus norvegicus* (Norway rat). Our results showed that adaptive selection has contributed to the genetic diversification of these proteins in murine lineage. Moreover, in both *M. musculus* and *R. norvegicus*, the chemokine and its receptor exhibit similar signs of selective sweeps resulting from positive selection. In light of currently available structural and interaction information for chemokines and their receptors, the similarity of XCL1/XCR1 evolutionary patterns among murine species and the parallels of their evolutionary footprints within individual species suggest that interplay could exist between the adaptively selected changes, or between the domains on which the identified changes are located, and consequently preserve the physiological interaction of XCL1 and XCR1.

1. Introduction

The host's immune system is composed of many cell types that collectively defend the body against pathogens, including parasites, fungi, bacteria, and viruses, as well as the growth of cancerous cells. The migration of immune cells to the site of immune surveillance plays pivotal roles in immune responses (Springer, 1995). Furthermore, motility of these cells forms the basis for their development within specific microenvironments (Masopust and Schenkel, 2013; Mosser and Edwards, 2008; Randolph et al., 2008; Schumacher et al., 2010; Shi and Pamer, 2011; Sun and Lanier, 2011). It has been well recognized that members of the chemokine superfamily, including a large number of chemokines and their adhesion receptors, function as critical regulators for the function and organization of these immune responses system (Allen et al., 2007; Zlotnik and Yoshie, 2012).

Chemokines are small proteins and characterized by their four cysteines (Zlotnik and Yoshie, 2000, 2012). Two disulfide bonds are formed between the first and the third cysteine residues and between the second and the fourth ones. The chemokine family consists of approximately 50 peptides in humans, with homologs and related peptides in other vertebrate species (Nomiyama et al., 2013; Proudfoot and Mariagrazia, 2016; Zlotnik and Yoshie, 2012). Chemokines are generally categorized into four subfamilies, i.e., CX3C, CXC, CC, and C (or XC), primarily based on the arrangement of the N-terminal conserved cysteine (C) residues (Zlotnik and Yoshie, 2000, 2012). The C subfamily lacks the first and the paired third cysteine. Another type of chemokine, which was termed the CX subfamily, has been identified only in zebrafish (Nomiyama et al., 2008). In the CX chemokines, one of the two N terminus cysteines is missing but the third and fourth ones are retained. The three-dimensional structures of a number of chemokines have been described (Allen et al., 2007; Nguyen and Vogel, 2012). Despite large differences in amino acid sequences, they preserve similar structures, which consist of a disordered N-terminal loop, a central three-stranded antiparallel β-sheet, and a C-terminal α-helix.

In the leukocyte migration during the immune surveillance and activation, the function of chemokines requires the presence of their

* Corresponding author. College of Animal Science and Technology, Sichuan Agricultural University, Wenjiang, Chengdu, 611130, People's Republic of China.
E-mail address: liyan@sicau.edu.cn (Y. Li).
[1] These authors contributed equally for this work.

https://doi.org/10.1016/j.dci.2019.04.008
Received 17 February 2019; Received in revised form 21 April 2019; Accepted 21 April 2019
Available online 23 April 2019
0145-305X/

complementary cell-surface receptors (Charo and Ransohoff, 2006; Rot and von Andrian, 2004). There are approximately 20 chemokine receptors identified in human to date, which are grouped into four subfamilies according to category of their major chemokine ligands (Bacon et al., 2002; Zlotnik and Yoshie, 2012). Sequence analysis indicated that these receptors are G-protein-coupled seven transmembrane receptors (Baldwin, 1994; de Brevern et al., 2005; Paterlini, 2002). The interaction of chemokines with their receptors results in induction of intracellular signals, which consequently promotes directional cellular migration and a range of physiological and pathological processes (Allen et al., 2007).

The chemokine XCL1 (also known as lymphotactin, SCM-1, ATAC) is the only member of the C chemokine subfamily in the house mouse (*Mus musculus*) (Kelner et al., 1994; Kennedy et al., 1995; Muller et al., 1995; Yoshida et al., 1995). In human, there are two homologues, XCL1 and XCL2, with only two amino acid differences from each other (Fox et al., 2015; Zlotnik and Yoshie, 2012). Human XCL1s and mouse XCL1 share 60% amino acid identity (Kennedy et al., 1995). Structurally, in contrast with other chemokines, XCL1 has the unique property that adopts two distinct conformations in equilibrium (Tuinstra et al., 2008). One conformation, a monomeric chemokine-like fold (Ltn10), consists of an extended N-terminal loop, a three-stranded β-sheet, a helix, and a C-terminal highly disordered extension. Alternative conformation (Ltn40) adopts a four-stranded β-sheet topology without any α-helix and self-associates to form a dimer. During immune responses, the gene encoding XCL1 has been found to be expressed by natural killer (NK), $CD8^+$ T cells, $CD4^+$ T cells, NKT cells, γδ T cells, and thymic medullary epithelial cells (Lei and Takahama, 2012).

XCR1 has been found to be the only known receptor for XCL1 with binding and functional assays (Heiber et al., 1995; Shan et al., 2000; Yoshida et al., 1998). Similar to other chemokine receptors, XCR1 is a typical seven-transmembrane protein and can couple efficiently to G-proteins similar to other chemokine receptors (Yoshida et al., 1998). In mouse, the *XCR1* gene is exclusively expressed in cross-presenting $CD8^+$ dendritic cells (DCs), but not other DC subtypes, NK cells, granulocytes, monocytes, T cells, or B cells (Dorner et al., 2009). Further studies showed that, in human, the expression profile of *XCR1* is specifically expressed on $CD141^+$ ($BDCA3^+$) DCs, which are phenotypically homologous to $CD8^+$ DCs in mouse (Bachem et al., 2010; Crozat et al., 2010). In addition, this receptor is selectively expressed on $CD8^+$-like DCs in rhesus macaques, pig, and sheep (Crozat et al., 2010; Deloizy et al., 2016; Dutertre et al., 2014).

XCL1 and XCR1 play a crucial role in dendritic cells-mediated antigen cross-presentation (Bachem et al., 2010; Dorner et al., 2009; Kroczek and Henn, 2012). In bacterial, viral, and parasitic infections and autoimmune diseases, the expression of XCR1 is elevated in cross-presenting $CD8^+$ DCs in mouse and $CD141^+$ DCs in human, which are responsive to the chemoattraction toward XCL1 (Bachem et al., 2010; Dorner et al., 2009; Lei et al., 2011). The localized DCs take up antigen and present it by major histocompatibility complex class I (MHC-I) molecules to cytotoxic $CD8^+$ T lymphocytes (Bachem et al., 2012; den Haan et al., 2000; Pooley et al., 2001). The activated $CD8^+$ T cell subsequently attracted $XCR1^+$ DCs through elicits a rapid production of XCL1, as well as plasmacytoid DCs that can secrete high amounts of interferon (IFN) type I in a chemokine receptor CCR5-dependent manner to the site of $CD8^+$ T cell initial antigen recognition (Brewitz et al., 2017; Swiecki and Colonna, 2015). The co-localization of $XCR1^+$ DCs, $CD8^+$ T cells, and plasmacytoid DCs within a confined microenvironment optimizes the maturation of and cross-presentation by $XCR1^+$ DCs, enhancing the development of $CD8^+$ T cell response (Brewitz et al., 2017). It is noteworthy that the monomeric Ltn10 conformation, but not the dimeric Ltn40 conformation, serves as a functional XCR1 agonist in the process described above (Tuinstra et al., 2008).

In addition to the ability of chemoattraction in a receptor-dependent fashion, XCL1 can also bind to cell surface glycosaminoglycans (GAGs) promoting their retention on cell surfaces, which contributes to the establishment of concentration gradients. The XCL1 gradients provide directional signals for cellular migration and other cellular events (Fox et al., 2015; Peterson et al., 2004; Tuinstra et al., 2008). Besides GAG binding for the generation of chemokine gradient, XCL1 can directly interact with the HIV-1 envelope glycoprotein gp120 and then block HIV-1 attachment and entry (Guzzo et al., 2013, 2015). Also of note is that the Ltn40 conformation is the binding form responsible for GAG and gp120 interactions but fails to activate XCR1 (Guzzo et al., 2015; Tuinstra et al., 2008).

Despite the critical roles of XCL1/XCR1 in physiological processes, an increasing number of studies have demonstrated that they have multiple effects in a range of pathological events. For example, in mouse and patients with allergic asthma, the invariant natural killer T (*i*NKT) cell-mediated XCL1–XCR1 axis can recruit $CD103^+$ DCs into the lung and promote airway hyperresponsiveness (AHR) (Woo et al., 2018). Although the axis contributes anti-tumor immunity by recruiting DC cell into tumors (Böttcher et al., 2018), XCR1 could be over-expressed in breast cancer, lung cancer, oral cancer, and ovarian carcinoma, and promote cancer cell proliferation, adhesion, migration, and invasion through XCL1–XCR1-mediated chemoattraction (Gantsev et al., 2013; Khurram et al., 2010; Kim et al., 2012; Wang et al., 2015).

Although previous studies have provided insight on the critical roles of XCL1–XCR1 axis in immune responses, a comprehensive description is currently lacking as to the molecular interaction of XCR1 with XCL1. One reason we know little about their interaction is due to the intrinsic difficulties in studying membrane proteins (Rajagopalan and Rajarathnam, 2006; Schwartz, 1994). Of note, in evolutionary arms race, pathogens have evolved a range of anti-immune methods including a category of molecule mimics of the chemokines or/and chemokine receptors (Alcami and Lira, 2010; Epperson et al., 2012; Mantovani et al., 2006; Murphy, 2001). The pathogen-encoded mimics interact with host chemokines or/and chemokine receptors, thereby acting as a molecular trap to subvert and exploit the chemokine system. In terms of XCL1/XCR1, a number of pathogen-encoded proteins are characterized by chemokine-like or chemokine receptor-like properties (Catusse et al., 2008; Geyer et al., 2014; Lubman et al., 2014). They bind to likewise targets XCR1 or XCL1 and may consequently modulate the relevant immune responses. Obviously, corresponding changes in XCR1 and/or XCL1 could not only be valuable in understanding their strategies by which hosts and pathogens compete in the biological arms race, but perhaps more importantly also be a perfect introduction to their molecular interaction taking into consideration their ligand-receptor relationship.

Because human XCL1 and its receptor XCR1 exhibit high resemblance in expression pattern and immune responses with their homologues in mouse, sheep, pig, and rhesus macaque, they are generally regarded as functionally conserved proteins across species (Lei and Takahama, 2012; Yamazaki et al., 2010; Yoshida et al., 1995). Therefore, in the present study, we analyzed the genetic variations of *XCL1* and *XCR1* among model organisms, *M. musculus* and *Rattus norvegicus*, and twelve other murine rodent species to describe their evolutionary pattern. The genetic diversity of these genes might provide valuable information about their evolutionary trajectories at multiple time intervals and facilitate elucidation of their evolutionary features. Furthermore, we performed allelic comparisons of these genes in *M. musculus* and *R. norvegicus* to find out more about their evolutionary significance.

2. Materials and methods

2.1. Samples

To provide comprehensive information about the evolutionary patterns of *XCL1* and *XCR1* in the rodent subfamily Murinae, we obtained samples from twelve species (Table S1). The sequences of *M.*

musculus (strain C57BL/6) and *R. norvegicus* (strain Sprague-Dawley) were obtained from GenBank. To understand the intraspecific changes in the genes, fourteen individuals of *R. norvegicus* and nine *M. musculus* were sampled from geographically distant points. Full details of our taxonomic sampling are in Tables S1 and S2.

2.2. DNA sequencing and alignment

The entire *XCL1* and *XCR1* gene sequences of non-mouse and non-rat species were amplified from genomic DNA. Because a number of primers have been used which are capable of amplifying the entire coding region from different species, primer sequences are available upon request. The products of PCR amplification were purified and cloned using the pMD 19-T Vector kit (TaKaRa). The inserts were sequenced using the vector primers. The coding regions of the sequences from these samples were defined based on their GenBank entries of *M. musculus* and *R. norvegicus*. Combined with that of *M. musculus* and *R. norvegicus*, the resulting sequences were aligned using ClustalW (Thompson et al., 1997) and checked manually. With regard to intraspecific variation, we sequenced the complete coding sequences of *XCL1* and *XCR1* in 23 individuals from *M. musculus* and *R. norvegicus* (Table S2). Additionally, for the same *M. musculus* and *R. norvegicus* individuals, 500bp intron sequences in the 5′-flank of the *XCL1* 2nd exons were sequenced for Tajima's test (see below) (Table S2). All of the intraspecific datasets were aligned with the methods outlined above.

2.3. Modeling

Because no three-dimensional structure of murine XCL1 and XCR1 has to date been reported, their structural information were predicted with their amino acid sequences from *M. musculus*. Because a seven transmembrane helices arrangement is a hallmark of chemokine receptors, a scan for XCR1 transmembrane helices was conducted using the TMHMM Server (http://www.cbs.dtu.dk/services/TMHMM/) (Krogh et al., 2001). For XCL1, we simulated its three-dimensional structure with SWISSMODEL (Automated Protein Modeling Server https://www.swissmodel.expasy.org/) (Biasini et al., 2014; Bordoli et al., 2009). The three-dimensional structure confidence (QMEAN Z-score) was assessed using Structure Assessment (Benkert et al., 2011).

2.4. Comparisons of synonymous and nonsynonymous variation rates

To evaluate adaptive selection acting on *XCL1* and *XCR1* in murines, we first analyzed the substitution patterns between pairs of species. Using their complete coding sequences from 14 rodent species (Table S1), we assayed the ratio of the number of non-synonymous substitutions per non-synonymous site (d_N) and the number of synonymous substitutions per synonymous site (d_S) for each gene with Pamilo-Bianchi-Li's method (Li, 1997). With regard to *XCR1*, because the extracellular, cytoplasmic, and transmembrane portions could preserve distinct structures and perform different functions in physiological processes, we further calculated the ratios of d_N and d_S for these regions separately using the methods outlined above (Table S3 in Supporting Information). The Z-test was adopted to detect deviations of d_N/d_S from neutrality ($d_N/d_S = 1$) (Nei and Kumar, 2000). A d_N/d_S ratio that exceeds one significantly indicates adaptive selection, while a $d_N/d_S < 1$ reflects negative selection.

In order to investigate the evolutionary pattern of *XCL1* and *XCR1* in *M. musculus* and *R. norvegicus*, we computed the ratio of the number of nonsynonymous polymorphisms per nonsynonymous site (p_N) and that of the number of synonymous polymorphisms per synonymous site (p_S) for each gene from both species (Table S2). Because of the relatively small numbers of polymorphisms in these datasets, Fisher's exact test (two-tailed) of independence was implemented for statistical evaluation (McDonald, 2009a; Zhang et al., 1997).

2.5. The maximum likelihood (ML) analysis of XCL1 and XCR1

Using the complete coding sequences of *XCL1* and *XCR1* from 14 rodent species (Table S1), we detected the impact of adaptive selection at their individual amino acid sites with CODEML in the PAML package (Yang, 1997, 2007). We implemented two pairs of models, M7 versus M8 and M8a versus M8, into generating two likelihood ratios. The null models M7 and M8a assume that all codons evolved neutrally or under purifying selection (d_N/d_S values ≤ 1); the alternative model M8 allows a proportion of sites to be under adaptive selection with d_N/d_S values > 1. For each paired comparison, a likelihood ratio test (LRT) was employed to compare the two models with and without adaptive selection (Nielsen and Yang, 1998; Swanson et al., 2003; Zhang et al., 2005). Under model M8, posterior probabilities were calculated with a empirical Bayes approach to identify the amino acid sites influenced by adaptive selection (Yang et al., 2005).

2.6. Tajima's test

For each intraspecific dataset, Tajima's test was implemented to examine whether the DNA polymorphism pattern conforms to the neutral mutation expectation (Tajima, 1989). Tajima's *D* is a statistic for measuring the difference between θ, which is based on the number of segregating sites, and π, the average number of pairwise differences (Nei, 1987; Watterson, 1975). Under neutrality, these two measures should be identical and Tajima's *D* value is expected to be zero. If the population experienced natural selection, background selection, or bottleneck recently, newly arisen mutations will be disproportionately present with low frequency or even as singletons, which will cause Tajima's *D* value to be negative (Slatkin and Hudson, 1991; Tajima, 1989). In this study, we calculated θ, π, and Tajima's *D* values using the program DNAsp, version 5 (Librado and Rozas, 2009). Additionally, Tajima's *D* on synonymous variations (D_{Syn}) and Tajima's *D* on non-synonymous variations (D_{Non}) were computed separately for these allelic datasets using the same method (Librado and Rozas, 2009; Wise et al., 1998).

3. Results

3.1. The evolutionary patterns of XCL1 and XCR1 in murine rodents

The molecular signature of evolutionary process can be identified through comparative nucleotide sequence analysis along a phylogeny. In order to provide a clear evolutionary pattern of *XCL1* and *XCR1* for the rodent subfamily Murinae, we analyzed the genetic variations of these genes in fourteen species (Table S1 in Supporting Information). The d_N/d_S ratios of the entire coding region in pairwise comparisons were calculated for each gene and the Z-test was performed for detecting deviation from neutrality. For *XCL1*, we observed that d_N exceeded d_S significantly in *M. musculus* versus *Apodemus agrarius* ($P = 0.008$) and *M. musculus* versus *A. draco* ($P = 0.030$). In addition, the d_N/d_S ratios of 36 pairwise comparisons were larger than 1, which deviated from neutral expectation (Fig. 1a). For *XCR1*, the Z-test showed that none of the d_N/d_S ratios exceeded one significantly (Fig. 1b). It is noteworthy that the different portions (extracellular, transmembrane, and cytoplasmic domains) of transmembrane proteins, such as MHCI and Toll-Like Receptors display different genetic variation patterns (Hughes and Nei, 1988; Wlasiuk and Nachman, 2010). Therefore, we performed further analyses for the individual domains separately. In the first instance, TMHMM analysis was implemented to scan for transmembrane helices (Krogh et al., 2001). The result clearly showed the locations of the seven transmembrane helices in the primary sequence of XCR1, which are general consistent with the information of ENSEMBL (www.ensembl.org) and available results (Yoshida et al., 1999) (Table S3 in Supporting Information). We then calculated the d_N/d_S ratios for three data subsets representing the

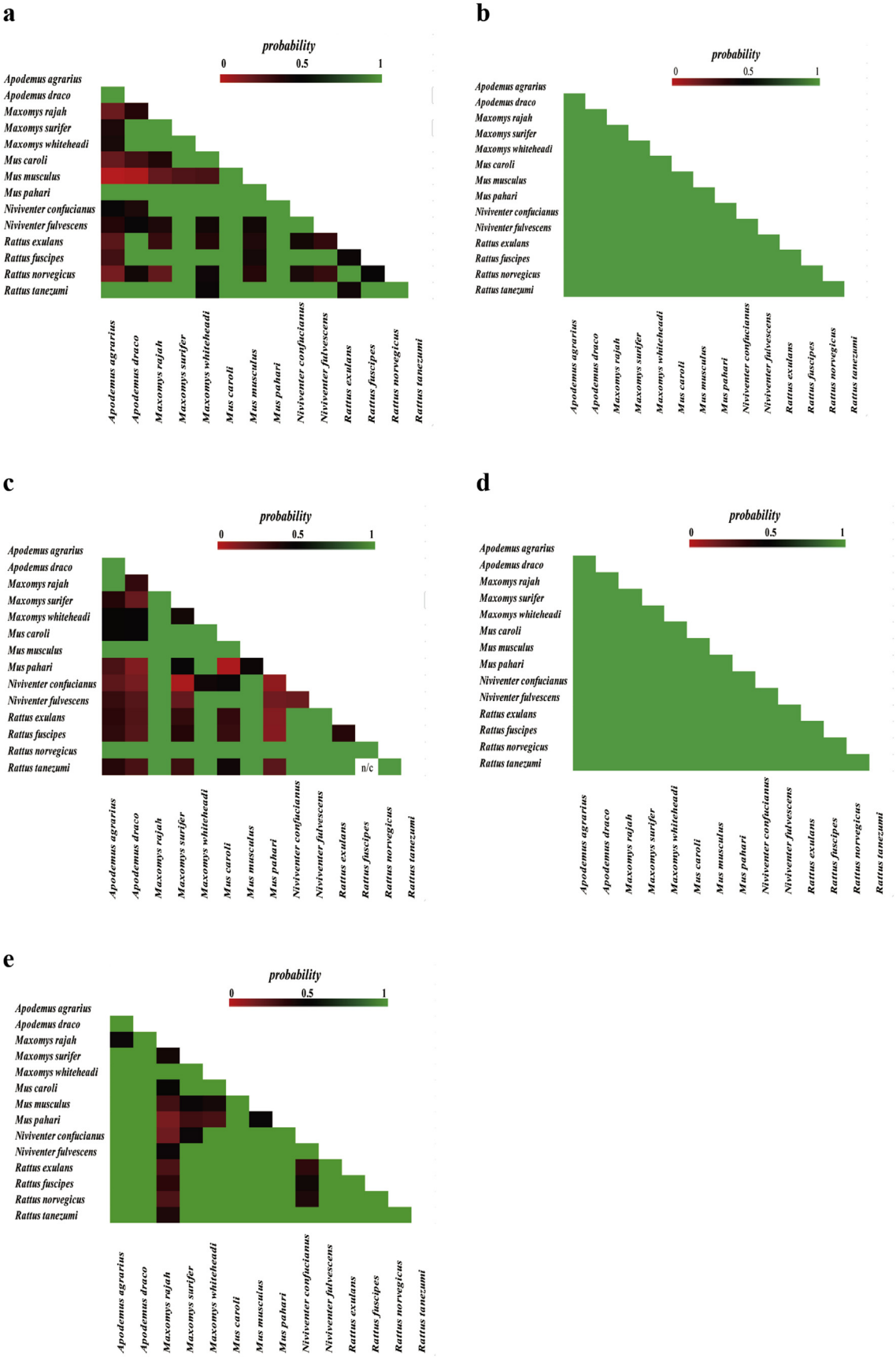

Fig. 1. Matrix of Z-test-statistics for pairwise nonsynonymous versus synonymous substitution ratios (d_N/d_S). The heatmaps are color-coded to represent probabilities at which the null hypothesis ($d_N = d_S$) cannot be rejected and depend on the alternative hypothesis of positive selection ($d_N > d_S$, lower left) from the full-length *XCL1*s (a) and *XCR1*s (b), and the extracellular (c), transmembrane (d), and cytoplasmic (e) portions of *XCR1*s. (For interpretation of the references to color in this figure legend, the reader is referred to the Web version of this article.)

extracellular, transmembrane, and cytoplasmic regions (Fig. 1c–e). For the transmembrane regions, none of the pairwise comparison ratio was $d_N/d_S > 1$ significantly, which is consistent with the observation of the entire coding region (Fig. 1d). By comparison, for the extracellular regions, the ratios of *Maxomys surifer* versus *Niviventer confucianus* ($P = 0.038$) and *M. caroli* versus *M. pahari* ($P = 0.036$) were significantly greater than one. *Apodemus draco* versus *M. pahari* exceeded one with a marginally significant probability ($P = 0.067$). Furthermore, the d_N value exceeded that of d_S in 40 of the rest pairwise comparisons (Fig. 1c). For the cytoplasmic regions, similar to that of extracellular domain, the d_N/d_S ratios of 20 pairwise comparisons were larger than 1 although the deviations were not statistically significant (Fig. 1e). Taken together, these results clearly suggest that adaptive selection has influenced the variation of *XCL1* and *XCR1* in murine rodent lineages.

3.2. Signature of adaptive selection on the individual amino acids of XCL1 and XCR1

Adaptive selection typically operates on few amino acid sites of a protein, as a major proportion of amino acids are under functional constraints (Li, 1997). Thus, using a codon-based test in a maximum likelihood framework (Yang, 1997, 2007), we detected the individual amino acid changes that were influenced by adaptive selection in *XCL1* and *XCR1* during Murinae evolution. For *XCL1*, the LRT of M8 versus M8a showed that the model endowed with positive selected sites ($d_N/d_S > 1$) fits the data significantly better than the model for neutrality or under purifying selection ($d_N/d_S \leq 1$) (Table 1). Although the LRT of M8 versus M7 was not significant, the value of log-likelihood difference (-2ΔL) indicated that the alternative model for adaptive selection fits the data better than the null models with a probability over 0.90 (x^2 distribution with d.f. = 2). The BEB analysis indicated that two amino acid sites (16 and 94) had d_N/d_S ratios exhibiting a departure from neutrality in favor of adaptive selection ($P > 0.95$). Moverover, site 79 showed $d_N/d_S > 1$ with a posterior probability over 0.9. For *XCR1*, the results of LRTs showed that the model with adaptively selected sites matches the data significantly better than the null models in both comparisons (Table 1). Four sites (36, 185, 187, and 270) were subject to adaptive selection ($P > 0.95$) and two sites (255 and 308) exhibited such signature at the $P > 0.90$ level (Table 1). These results suggest that adaptive selection played an important role in shaping rapid amino acid variations at these sites.

To further understand the structural and functional significance of the evolutionary changes, we looked at the location of the adaptively selected amino acid sites in their structural models. Since XCL1 adopts two distinct structures, Ltn10 and Ltn40 conformations, we simulated the tertiary structures of both conformations (Table 1 and Fig. 2) (Dorner et al., 1997). Pairwise alignments of mouse XCL1 against human template showed that they share high sequence identity (about 60%), which confirmed that the determined structures of the templates could be used for modeling. The reliability of modeling was assessed, and the resulting QMEAN4 Z-scores are −1.58 for Ltn10 conformation and −4.05 for Ltn40 conformation. We then located the identified amino acid sites 79 and 94 (correspond to sites 58 and 73 of the mature peptide region), except for site 16 in the removed signal peptide. On the structural models of the Ltn10 conformation, site 79 is located on the α-helix, as is site 94 on the C-terminal highly disordered extension (Fig. 2a) (Kuloglu et al., 2001). On the Ltn40 conformation, the identified sites are located on the C-terminal highly disordered extension following four-stranded β-sheet (Fig. 2b) (Tuinstra et al., 2008). For XCR1, based on the basic structural fold, the identified sites fall in different domains: one group of sites (36, 185, 187, and 270) lies in the extracellular N-terminal segment and loops (exoloops) (Table 1 and Fig. 3); one site (255) lies in the sixth transmembrane helix (Table 1 and Fig. 3); another site (308) lies in the cytoplasmic C-terminal segment (Table 1 and Fig. 3).

3.3. Signature of adaptive selection on the evolution of XCL1 and XCR1 in M. musculus and R. norvegicus

Because *M. musculus* is the most commonly used mammalian model for the study of *XCL1* and *XCR1*, we analyzed the genetic variations of these genes in mouse as well as in another important mammalian model *R. norvegicus* to shed further insights into their evolution. We first performed an allelic comparison of DNA sequence polymorphisms with each of *XCL1* and *XCR1* datasets from *M. musculus* and *R. norvegicus* (Table S2). In possible pairwise comparisons, the p_N/p_S ratios were calculated and deviations of the ratio values from neutrality were statistically inferred with Fisher's exact test (Fig. S1) (McDonald, 2009b; Zhang et al., 1997). None of the pairwise comparison ratios is larger or smaller than one significantly, although *XCR1*s have shown an excess of nonsynonymous variation relative to the number of silent in *M. musculus* (19 versus 5) and *R. norvegicus* (33 versus 9) (Table S4). Of note, the *XCL1* and *XCR1* harbored polymorphisms are mainly present as singleton in both species. For *XCL1*, all nucleotide polymorphisms in *M. musculus* and the majority of polymorphic variations (10 of 12) in *R. norvegicus* are singletons (Table 2). Similarly, for *XCR1*, the majority of nucleotide polymorphisms in these species are also singletons (*M. musculus*, 23 of 24; *R. norvegicus*, 34 of 41) (Table 2). The disproportionate presences of the singletons infer that recent selective sweeps, driven by positive selection, might have influenced the genetic variations of *XCL1* and *XCR1* in both species. To evaluate the plausibility of the assumption, we then performed Tajima's test with these *XCL1* and *XCR1* allelic datasets. For each dataset, we observed that θ exceeded π and caused negative Tajima's *D* value with significant difference from

Table 1
Likelihood values and sites inferred to be under positive selection for *XCL1* and *XCR1* genes in murine rodents.

Gene	Model	l[a]	-2ΔL[b]	Sites under selection identified by PAML
XCL1				
	M7: beta	−1227.32	5.12 (M8 versus M7)	Not allowed
	M8a: beta & fixed ω	−1227.28	5.04* (M8 versus M8a)	Not allowed
	M8: beta & ω	−1224.76		16, 94 (at $P \geq 0.95$)
				79 (at $0.95 > P \geq 0.90$)
XCR1				
	M7: beta	−3409.85	24.80** (M8 versus M7)	Not allowed
	M8a: beta & fixed ω	−3407.89	20.88** (M8 versus M8a)	Not allowed
	M8: beta & ω	−3397.45		270 (at $P \geq 0.99$)
				36, 185, 187 (at $0.99 > P \geq 0.95$)
				255, 308 (at $0.95 > P \geq 0.90$)

Single and double asterisks correspond to $P < 0.05$ or $P < 0.01$, respectively (one-tailed *t*-test). The numbers of amino acid sites represent their position in the mouse XCL1 and XCR1 sequence.

[a] l = the log likelihood value under different codon-based model.

[b] -2ΔL = twice the log likelihood difference between pair of models.

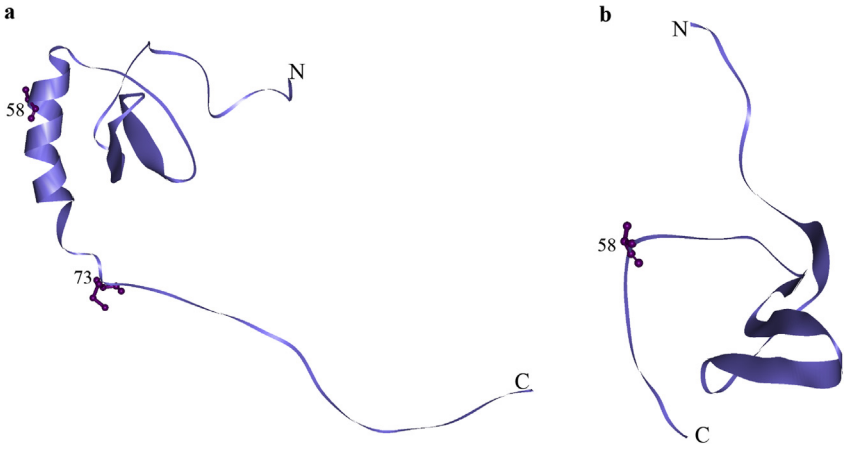

Fig. 2. Locations of divergence-related amino acid sites in the stick models of (a) XCL1 Ltn10 conformation (template PDB ID: 1j9o) and (b) XCL1 Ltn40 conformation (template PDB ID: 2n54). Numbers associated with colored points are the amino acid positions in the mature peptide region *Mus musculus* full-length XCL1 (NM_008510). In (b), there is one amino acid (73) missing due to its absence in the template.

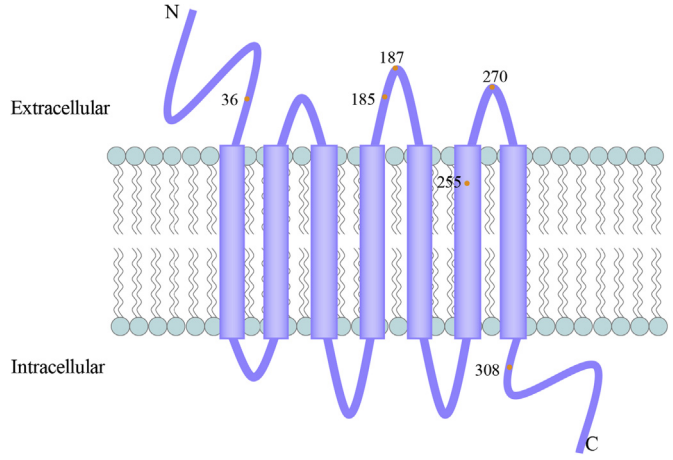

Fig. 3. Locations of divergence-related amino acid sites in the stick models of XCR1. Numbers associated with colored points are the amino acid positions in *Mus musculus* XCR1 (NM_011798).

zero (Table 2). These statistics support our hypothesis that *XCL1* and *XCR1* might have been influenced by recent selective sweep in *M. musculus* and *R. norvegicus*.

It is noteworthy that the negative values of *D* can also be explained by recent background selection or bottleneck (Charlesworth et al., 1993; Tajima, 1989). In the case of background selection, non-deleterious variations can be purged by strong negative selection due to spatial proximity to deleterious alleles. Consequently, it reduces intraspecific diversity and yields the pattern of singleton and the statistic in Tajima's test similar to those of selective sweep (Li, 1997). In terms of *XCL1* and *XCR1*, however, the reductions in variation are not likely due to background selection (negative selection) because of the following. (i) The statistical results indicated that the adaptive selection has contributed remarkably to their evolution in the explosion process of murine taxa (Fig. 1 and Table 1). When closely viewed from the perspective of *M. musculus* and *R. norvegicus*, a similar evolutionary pattern is visible on both genes. Concretely, for *XCL1*, d_N exceeded d_S significantly in *M. musculus* versus *A. Agrarius* and *M. musculus* versus *A. draco*. Moreover, the d_N/d_S ratios of eight comparisons between *R. norvegicus* and other species were larger than one although the deviations were not statistically significant (Fig. 1a). For the cytoplasmic region of *XCR1*, there were four and two pairwise comparisons involving *M. musculus* or *R. norvegicus* that respectively exceeded one (Fig. 1e). In addition, for the extracellular region of this gene, the d_N/d_S ratios of four comparisons involving *M. musculus* were larger than one (Fig. 1c). (ii) For the *XCR1* allelic comparisons of *M. musculus* and *R. norvegicus*, p_N exceeded p_S in a number of allelic pairwise comparisons although none of the ratio values is larger than one significantly (Fig. S1c and d). For those of the *M. musculus* and *R. norvegicus XCL1*s, the statistics of the p_N/p_S ratios also failed to reject a null hypothesis of neutrality. Furthermore, if there had been recent negative selection on these alleles, we would not expect to observe reductions of synonymous polymorphism because they are neutral and can be incorporated into the population. However, Tajima's *D* values on synonymous sites (D_{syn}) are significantly negative in all allelic datasets of *XCL1* and *XCR1* (Table S2). Thus, at the intraspecific level, negative selection does not adequately explain the results of Tajima's test. On the whole, the combined results from inter- and intraspecies analyses suggested that the reductions of variation detected at these genes are unlikely to be explained by negative selection. A bottleneck, a single period of small population, can result in a loss in genetic heterozygosity for the different genomic regions while a selective sweep reduces heterozygosity at a specific locus (Hamblin and Rienzo, 2000; Hartl and Clark, 1997; Li, 1997). In

Table 2
Nucleotide diversity of *XCL1* and *XCR1* in *Mus musculus* and *Rattus norvegicus*.

Region	No. nucleotide sites (bp)	*Mus musculus*				*Rattus norvegicus*			
		S^a	π^b	θ^c	Tajima's *D*	*S*	π	θ	Tajima's *D*
Coding sequence									
XCL1	342	5 (5)	1.62	4.25	−1.956*	12 (10)	3.07	9.02	−2.184**
XCR1	1014	24 (23)	3.07	7.13	−2.326**	41 (34)	3.41	10.64	−2.541**
Partial *XCL1* 1st intron	500	10 (9)	3.01	5.83	−1.739	30 (21)	9.17	15.45	−1.488

*P < 0.05.
**P < 0.01.
[a] The number of segregating sites.
[b] The average number of pairwise differences per site between sequences. All values are multiplied by 10^3.
[c] The average number of segregating nucleotide sites among all sequences. All values are multiplied by 10^3.

this context, using Tajima's test, we analyzed the intronic sequences in the 5′-flank region of the *XCL1* 2nd exons from the same *M. musculus* and *R. norvegicus* specimens. No significant results were obtained for both allelic datasets that differ from those identified in the coding sequences, although they are in close spatial proximity (Table 2). Thus, the incongruences of the statistics among the genomic regions indicate that the reductions in variation of *XCL1* and *XCR1* coding sequences are unlikely to be explained by bottleneck. Taken together, from these lines of evidence, it is reasonable to suggest that the evolutions of *XCL1* and *XCR1* in *M. musculus* and *R. norvegicus* have been influenced, at least in part, by recent selective sweep.

4. Discussion

This study investigated the evolution of *XCL1* and *XCR1* in murine rodents. Interspecific and intraspecific comparisons shed insights into their evolutionary trajectories and functional divergence acting over different timescales. The results suggested that adaptive selection had played an important role in shaping the evolution of these genes and contributed to the changes at a number of sites (Table 1). Of note, *XCL1* and *XCR1* exhibit clear signatures not only of concordant evolutionary pattern in the expansion of the murines, but also of co-occurrent selective sweep both in *M. musculus* and *R. norvegicus*. The existence of such evolution features led to the proposal that the *XCL1* and *XCR1* underwent adaptive evolution along parallel trajectories in murine rodents. In this scenario, it is reasonable that the adaptive changes at sites 79 (which lies in the α-helix) and 94 (which lies in the C-terminal extension) might favor the interaction of XCL1 Ltn10 conformation with its receptor XCR1. In support of this hypothesis, it has been observed that the truncated variants of XCL1 which is missing the C-terminal 21- or 22-amino acid extension showed no activity for XCL1–XCR1 axis (Hedrick et al., 1997; Marcaurelle et al., 2001).

It is further noteworthy that, under the above outlined hypothesis, our results on XCR1 might provide clues to the molecular details of its recognition mode for XCL1. With respect to ligand binding of seven-transmembrane receptor, a two-step model has been proposed in which multiple domains of the receptor are involved in binding the ligand (Monteclaro and Charo, 1996; Schwartz, 1994). Consistently with the model, the structure-function studies have shown that chemokine ligand-receptor binding interaction involves two sites: the chemokine N-terminus and chemokine receptor extracellular N-terminus (site-I), and the chemokine N-terminus and the receptor one or more exoloops and transmembrane domains (site-II) (Monteclaro and Charo, 1996; Rajagopalan and Rajarathnam, 2006; Scholten et al., 2012). However, because seven-transmembrane receptors and ligands may interact in vastly different manners, further case-by-case studies are necessary to fully comprehend the context-specific binding interaction (Rajagopalan and Rajarathnam, 2006; Schwartz, 1994). Of note, previous studies have revealed that seven-transmembrane receptors and ligands may interact in vastly different manners (Rajagopalan and Rajarathnam, 2006; Schwartz, 1994). For example, the N-terminus of the chemokine MCP-1/CCL2 receptor is necessary for high affinity binding of MCP-1, and that other regions of the receptor are required to mediate signal transduction. In contrast, binding and signal transduction induced by the chemokine MIP-1a/CCL3 do not appear to require the N-terminus, but do require the presence of the third exoloop of its receptor C−C CKR-1 (Monteclaro and Charo, 1996). Hence, further case-by-case studies are necessary to fully comprehend the context-specific binding interaction. In our results, the adaptively selected sites are located on different structural domains (Fig. 3). Site 36 is located on the extracellular N-terminal segment. Sites 185, 187, and 270 are separately located on the second and third exoloops. Site 255 is located on the sixth transmembrane helix, as is site 308 in the cytoplasmic C-terminal segment. In combination with the similar evolutionary fates of XCR1 and its counterpart, the distribution pattern of identified sites implies that these sites and corresponding segments (N-terminus, the sixth transmembrane helix, and the second and third exoloops) could be participating in interaction with XCL1 (Fig. 3). In the context of the two-step model, the N-terminal segment of XCR1 might serve as one site to position XCL1, and the second and/or third exoloops, in cooperation with the sixth transmembrane helix, might form a pocket as a second site that binds the ligand and ultimately initiates chemotaxis.

In conclusion, our analyses provide evidence that adaptive selection has contributed to the changes of *XCL1* and *XCR1* in an important group of mammals, murine rodents. From the perspective of evolution, these adaptive changes constitute functional adaptations, most likely in a concordant manner, to counter endogenous changes or microbial insults towards XCL1–XCR1 axis. Because XCL1 and XCR1 could have coped with respective endogenous and/or exogenous challenges in different animal groups, it is necessary to study their evolutionary features in other phylogenic lineages, such as fishes. Fishes represent more than one half of all vertebrate species and are the first that present adaptive immune mechanisms (Litman et al., 2005; Nelson, 2006). In zebrafish, an important experimental model, a single C chemokine has been identified based on a systematic search (Nomiyama et al., 2008). The tendency of *XCL1* to act on single or low copy number genes in remarkably diverse groups of the vertebrates inferred that they might exist prior to the split of these phylogenic lineages. However, the zebrafish *XCL* shows little homology to mammalian C chemokines and is phylogenically clustered with the fish CC rather than the mammalian C subfamily members (Nomiyama et al., 2008). Therefore, taking into consideration the presence of adaptive diversification at *XCL1* in mammals, further evolutionary analyses of fish C chemokines and their receptors will be invaluable not only in characterizing their origination and evolutionary trajectories, but also in gaining deep insight into their functional signatures in the confrontation with the challenges of different environments.

From the perspectives of structure and function, such evolution signatures provide hints about the molecular mechanism of the interaction between XCL1 and XCR1. Certainly, further studies are needed to validate the structural and functional implication(s). If the inferences are experimentally supported, they would shed more insight not only into their versatile roles under physiological and pathological conditions, but also into the development of receptor agonists and antagonists for the treatment of human diseases relevant to XCL1 and/or XCR1.

Funding source

Y. L. wishes to thank Sichuan Agricultural University for financial support.

Conflicts of interest

The authors declare that they have no conflict of interest.

Acknowledgements

We thank Annie Orth for providing the *Mus pahari* sample. We are grateful to Vernon Tintinger for providing the *Rattus exulans*, *R. fuscipes*, and *R. tanezumi* DNA samples. We are indebted to Yu-Teh Kirk Lin for providing the *M. caroli* samples. We also thank University of Michigan Museum of Zoology for providing the *Maxomys rajah*, *M. surifer*, and *M. whiteheadi* samples.

Appendix A. Supplementary data

Supplementary data to this article can be found online at https://doi.org/10.1016/j.dci.2019.04.008.

References

Alcami, A., Lira, S.A., 2010. Modulation of chemokine activity by viruses. Curr. Opin. Immunol. 22, 482–487.

Allen, S.J., Crown, S.E., Handel, T.M., 2007. Chemokine: receptor structure, interactions, and antagonism. Annu. Rev. Immunol. 25, 787–820.

Böttcher, J.P., Bonavita, E., Chakravarty, P., Blees, H., Cabeza-Cabrerizo, M., Sammicheli, S., Rogers, N.C., Sahai, E., Zelenay, S., Reis e Sousa, C., 2018. NK cells stimulate recruitment of cDC1 into the tumor microenvironment promoting cancer immune control. Cell 172, 1022–1037 e1014.

Bachem, A., Guttler, S., Hartung, E., Ebstein, F., Schaefer, M., Tannert, A., Salama, A., Movassaghi, K., Opitz, C., Mages, H.W., Henn, V., Kloetzel, P.M., Gurka, S., Kroczek, R.A., 2010. Superior antigen cross-presentation and XCR1 expression define human CD11c+CD141+ cells as homologues of mouse CD8+ dendritic cells. J. Exp. Med. 207, 1273–1281.

Bachem, A., Hartung, E., Guttler, S., Mora, A., Zhou, X., Hegemann, A., Plantinga, M., Mazzini, E., Stoitzner, P., Gurka, S., Henn, V., Mages, H.W., Kroczek, R.A., 2012. Expression of XCR1 characterizes the batf3-dependent lineage of dendritic cells capable of antigen cross-presentation. Front. Immunol. 3, 214.

Bacon, K., Baggiolini, M., Broxmeyer, H., Horuk, R., Lindley, I., Mantovani, A., Maysushima, K., Murphy, P., Nomiyama, H., Oppenheim, J., Rot, A., Schall, T., Tsang, M., Thorpe, R., Van Damme, J., Wadhwa, M., Yoshie, O., Zlotnik, A., Zoon, K., 2002. Chemokine/chemokine receptor nomenclature. J. Interferon Cytokine Res. 22, 1067–1068.

Baldwin, J.M., 1994. Structure and function of receptors coupled to G proteins. Curr. Opin. Cell Biol. 6, 180–190.

Benkert, P., Biasini, M., Schwede, T., 2011. Toward the estimation of the absolute quality of individual protein structure models. Bioinformatics 27, 343.

Biasini, M., Bienert, S., Waterhouse, A., Arnold, K., Studer, G., Schmidt, T., Kiefer, F., Cassarino, T.G., Bertoni, M., Bordoli, L., Schwede, T., 2014. SWISS-MODEL: modelling protein tertiary and quaternary structure using evolutionary information. Nucleic Acids Res. 42, W252–W258.

Bordoli, L., Kiefer, F., Arnold, K., Benkert, P., Battey, J., Schwede, T., 2009. Protein structure homology modeling using SWISS-MODEL workspace. Nat. Protoc. 4, 1–13.

Brewitz, A., Eickhoff, S., Dähling, S., Quast, T., Bedoui, S., Kroczek, R.A., Kurts, C., Garbi, N., Barchet, W., Iannacone, M., 2017. CD8 + T cells orchestrate pdc-XCR1 + dendritic cell spatial and functional cooperativity to optimize priming. Immunity 46, 205–219.

Catusse, J., Spinks, J., Mattick, C., Dyer, A., Laing, K., Fitzsimons, C., Smit, M.J., Gompels, U.A., 2008. Immunomodulation by herpesvirus U51A chemokine receptor via CCL5 and FOG-2 down-regulation plus XCR1 and CCR7 mimicry in human leukocytes. Eur. J. Immunol. 38, 763.

Charlesworth, B., Morgan, M.T., Charlesworth, D., 1993. The effect of deleterious mutations on neutral molecular variation. Genetics 134, 1289–1303.

Charo, I.F., Ransohoff, R.M., 2006. The many roles of chemokines and chemokine receptors in inflammation. N. Engl. J. Med. 354, 610–621.

Crozat, K., Guiton, R., Contreras, V., Feuillet, V., Dutertre, C.A., Ventre, E., Vu Manh, T.P., Baranek, T., Storset, A.K., Marvel, J., Boudinot, P., Hosmalin, A., Schwartz-Cornil, I., Dalod, M., 2010. The XC chemokine receptor 1 is a conserved selective marker of mammalian cells homologous to mouse CD8alpha+ dendritic cells. J. Exp. Med. 207, 1283–1292.

de Brevern, A.G., Wong, H., Tournamille, C., Colin, Y., Le Van Kim, C., Etchebest, C., 2005. A structural model of a seven-transmembrane helix receptor: the Duffy antigen/receptor for chemokine (DARC). Biochim. Biophys. Acta 1724, 288–306.

Deloizy, C., Bouguyon, E., Fossum, E., Sebo, P., Osicka, R., Bole, A., Pierres, M., Biacchesi, S., Dalod, M., Bogen, B., 2016. Expanding the tools for identifying mononuclear phagocyte subsets in swine: reagents to porcine CD11c and XCR1. Dev. Comp. Immunol. 65, 31–40.

den Haan, J.M., Lehar, S.M., Bevan, M.J., 2000. CD8(+) but not CD8(-) dendritic cells cross-prime cytotoxic T cells in vivo. J. Exp. Med. 192, 1685–1696.

Dorner, B., Muller, S., Entschladen, F., Schroder, J.M., Franke, P., Kraft, R., Friedl, P., Clark-Lewis, I., Kroczek, R.A., 1997. Purification, structural analysis, and function of natural ATAC, a cytokine secreted by CD8(+) T cells. J. Biol. Chem. 272, 8817–8823.

Dorner, B.G., Dorner, M.B., Zhou, X., Opitz, C., Mora, A., Guttler, S., Hutloff, A., Mages, H.W., Ranke, K., Schaefer, M., Jack, R.S., Henn, V., Kroczek, R.A., 2009. Selective expression of the chemokine receptor XCR1 on cross-presenting dendritic cells determines cooperation with CD8+ T cells. Immunity 31, 823–833.

Dutertre, C.A., Jourdain, J.P., Rancez, M., Amraoui, S., Fossum, E., Bogen, B., Sanchez, C., CouëdelCourteille, A., Richard, Y., Dalod, M., 2014. TLR3-responsive, XCR1+, CD141(BDCA-3)+/CD8α+-equivalent dendritic cells uncovered in healthy and simian immunodeficiency virus-infected rhesus macaques. J. Immunol. 192, 4697.

Epperson, M.L., Lee, C.A., Fremont, D.H., 2012. Subversion of cytokine networks by virally encoded decoy receptors. Immunol. Rev. 250, 199–215.

Fox, J.C., Nakayama, T., Tyler, R.C., Sander, T.L., Yoshie, O., Volkman, B.F., 2015. Structural and agonist properties of XCL2, the other member of the C-chemokine subfamily. Cytokine 71, 302–311.

Gantsev, S.K., Umezawa, K., Islamgulov, D.V., Khusnutdinova, E.K., Ishmuratova, R.S., Frolova, V.Y., Kzyrgalin, S.R., 2013. The role of inflammatory chemokines in lymphoid neoorganogenesis in breast cancer. Biomed. Pharmacother. 67, 363.

Geyer, H., Hartung, E., Mages, H.W., Weise, C., Belužić, R., Vugrek, O., Jonjic, S., Kroczek, R.A., Voigt, S., 2014. Cytomegalovirus expresses the chemokine homologue vXCL1 capable of attracting XCR1+ CD4- dendritic cells. J. Virol. 88, 292–302.

Guzzo, C., Fox, J., Lin, Y., Miao, H., Cimbro, R., Volkman, B.F., Fauci, A.S., Lusso, P., 2013. The CD8-derived chemokine XCL1/lymphotactin is a conformation-dependent, broad-spectrum inhibitor of HIV-1. PLoS Pathog. 9 e1003852.

Guzzo, C., Fox, J.C., Miao, H., Volkman, B.F., Lusso, P., 2015. Structural determinants for the selective anti-HIV-1 activity of the all-β alternative conformer of XCL1. J. Virol. 89, 9061.

Hamblin, M.T., Rienzo, A.D., 2000. Detection of the signature of natural selection in humans: evidence from the duffy blood group locus. Am. J. Hum. Genet. 66, 1669–1679.

Hartl, D.L., Clark, A.G., 1997. Principles of Population Genetics. Sinauer associates Sunderland.

Hedrick, J.A., Saylor, V., Figueroa, D., Mizoue, L., Xu, Y., Menon, S., Abrams, J., Handel, T., Zlotnik, A., 1997. Lymphotactin is produced by NK cells and attracts both NK cells and T cells in vivo. J. Immunol. 158, 1533–1540.

Heiber, M., Docherty, J.M., Shah, G., Nguyen, T., Cheng, R., Heng, H.H., Marchese, A., Tsui, L.C., Shi, X., George, S.R., et al., 1995. Isolation of three novel human genes encoding G protein-coupled receptors. DNA Cell Biol. 14, 25–35.

Hughes, A.L., Nei, M., 1988. Pattern of nucleotide substitution at major histocompatibility complex class I loci reveals overdominant selection. Nature 335, 167–170.

Kelner, G.S., Kennedy, J., Bacon, K.B., Kleyensteuber, S., Largaespada, D.A., Jenkins, N.A., Copeland, N.G., Bazan, J.F., Moore, K.W., Schall, T.J., et al., 1994. Lymphotactin: a cytokine that represents a new class of chemokine. Science (New York, N.Y 266, 1395–1399.

Kennedy, J., Kelner, G.S., Kleyensteuber, S., Schall, T.J., Weiss, M.C., Yssel, H., Schneider, P.V., Cocks, B.G., Bacon, K.B., Zlotnik, A., 1995. Molecular cloning and functional characterization of human lymphotactin. J. Immunol. 155, 203–209.

Khurram, S.A., Whawell, S.A., Bingle, L., Murdoch, C., Mccabe, B.M., Farthing, P.M., 2010. Functional expression of the chemokine receptor XCR1 on oral epithelial cells †. J. Pathol. 221, 153.

Kim, M., Rooper, L., Xie, J., Rayahin, J., Burdette, J.E., Kajdacsy-Balla, A.A., Barbolina, M.V., 2012. The lymphotactin receptor is expressed in epithelial ovarian carcinoma and contributes to cell migration and proliferation. Molecular Cancer Research Mcr 10, 1419.

Kroczek, R.A., Henn, V., 2012. The role of XCR1 and its ligand XCL1 in antigen cross-presentation by murine and human dendritic cells. Front. Immunol. 3, 14.

Krogh, A., Larsson, B., Von, H.G., Sonnhammer, E.L., 2001. Predicting transmembrane protein topology with a hidden Markov model: application to complete genomes. J. Mol. Biol. 305, 567.

Kuloglu, E.S., Mccaslin, D.R., Kitabwalla, M., Pauza, C.D., Markley, J.L., Volkman, B.F., 2001. Monomeric solution structure of the prototypical 'C' chemokine lymphotactin. Biochemistry 40, 12486–12496.

Lei, Y., Ripen, A.M., Ishimaru, N., Ohigashi, I., Nagasawa, T., Jeker, L.T., Bosl, M.R., Hollander, G.A., Hayashi, Y., Malefyt Rde, W., Nitta, T., Takahama, Y., 2011. Aire-dependent production of XCL1 mediates medullary accumulation of thymic dendritic cells and contributes to regulatory T cell development. J. Exp. Med. 208, 383–394.

Lei, Y., Takahama, Y., 2012. XCL1 and XCR1 in the immune system. Microb. Infect./Institut Pasteur 14, 262–267.

Li, W.-H., 1997. Molecular Evolution. Sinauer Associates, Sunderland, MA.

Librado, P., Rozas, J., 2009. DnaSP v5: a software for comprehensive analysis of DNA polymorphism data. Bioinformatics 25, 1451–1452.

Litman, G.W., Cannon, J.P., Dishaw, L.J., 2005. Reconstructing immune phylogeny: new perspectives. Nat. Rev. Immunol. 5, 866.

Lubman, O.Y., Cella, M., Wang, X., Monte, K., Lenschow, D.J., Huang, Y.H., Fremont, D.H., 2014. Rodent herpesvirus Peru encodes a secreted chemokine decoy receptor. J. Virol. 88, 538–546.

Mantovani, A., Bonecchi, R., Locati, M., 2006. Tuning inflammation and immunity by chemokine sequestration: decoys and more. Nat. Rev. Immunol. 6, 907–918.

Marcaurelle, L.A., Mizoue, L.S., Wilken, J., Oldham, L., Kent, S.B., Handel, T.M., Bertozzi, C.R., 2001. Chemical synthesis of lymphotactin: a glycosylated chemokine with a C-terminal mucin-like domain. Chemistry 7, 1129–1132.

Masopust, D., Schenkel, J.M., 2013. The integration of T cell migration, differentiation and function. Nat. Rev. Immunol. 13, 309–320.

McDonald, J.H., 2009a. Handbook of Biological Statistics, third ed. Sparky House Publishing, Baltimore, Maryland.

McDonald, J.H., 2009b. Handbook of Biological Statistics. Sparky House Publishing Baltimore, MD.

Monteclaro, F.S., Charo, I.F., 1996. The amino-terminal extracellular domain of the MCP-1 receptor, but not the RANTES/MIP-1alpha receptor, confers chemokine selectivity. Evidence for a two-step mechanism for MCP-1 receptor activation. J. Biol. Chem. 271, 19084.

Mosser, D.M., Edwards, J.P., 2008. Exploring the full spectrum of macrophage activation. Nat. Rev. Immunol. 8, 958–969.

Muller, S., Dorner, B., Korthauer, U., Mages, H.W., D'Apuzzo, M., Senger, G., Kroczek, R.A., 1995. Cloning of ATAC, an activation-induced, chemokine-related molecule exclusively expressed in CD8+ T lymphocytes. Eur. J. Immunol. 25, 1744–1748.

Murphy, P.M., 2001. Viral exploitation and subversion of the immune system through chemokine mimicry. Nat. Immunol. 2, 116–122.

Nei, M., 1987. Molecular Evolutionary Genetics. Columbia University Press, New York.

Nei, M., Kumar, S., 2000. Molecular Evolution and Phylogenetics. Oxford University Press.

Nelson, J.S., 2006. Fishes of the World, fourth ed. John Wiley & Sons, New Jersey, USA.

Nguyen, L.T., Vogel, H.J., 2012. Structural perspectives on antimicrobial chemokines. Front. Immunol. 3, 384.

Nielsen, R., Yang, Z., 1998. Likelihood models for detecting positively selected amino acid sites and applications to the HIV-1 envelope gene. Genetics 148, 929–936.

Nomiyama, H., Hieshima, K., Osada, N., Kato-Unoki, Y., Otsuka-Ono, K., Takegawa, S., Izawa, T., Yoshizawa, A., Kikuchi, Y., Tanase, S., Miura, R., Kusuda, J., Nakao, M., Yoshie, O., 2008. Extensive expansion and diversification of the chemokine gene family in zebrafish: identification of a novel chemokine subfamily CX. BMC Genomics

9, 222.
Nomiyama, H., Osada, N., Yoshie, O., 2013. Systematic classification of vertebrate chemokines based on conserved synteny and evolutionary history. Genes Cells 18, 1–16.
Paterlini, M.G., 2002. Structure modeling of the chemokine receptor CCR5: implications for ligand binding and selectivity. Biophys. J. 83, 3012–3031.
Peterson, F.C., Elgin, E.S., Nelson, T.J., Zhang, F., Hoeger, T.J., Linhardt, R.J., Volkman, B.F., 2004. Identification and characterization of a glycosaminoglycan recognition element of the C chemokine lymphotactin. J. Biol. Chem. 279, 12598–12604.
Pooley, J.L., Heath, W.R., Shortman, K., 2001. Cutting edge: intravenous soluble antigen is presented to CD4 T cells by CD8- dendritic cells, but cross-presented to CD8 T cells by CD8+ dendritic cells. J. Immunol. 166, 5327.
Proudfoot, A.E.I., Mariagrazia, U., 2016. Modulation of chemokine responses: synergy and cooperativity. Front. Immunol. 7.
Rajagopalan, L., Rajarathnam, K., 2006. Structural basis of chemokine receptor function–a model for binding affinity and ligand selectivity. Biosci. Rep. 26, 325–339.
Randolph, G.J., Ochando, J., Partida-Sanchez, S., 2008. Migration of dendritic cell subsets and their precursors. Annu. Rev. Immunol. 26, 293–316.
Rot, A., von Andrian, U.H., 2004. Chemokines in innate and adaptive host defense: basic chemokinese grammar for immune cells. Annu. Rev. Immunol. 22, 891–928.
Scholten, D.J., Canals, M., Maussang, D., Roumen, L., Smit, M.J., Wijtmans, M., de Graaf, C., Vischer, H.F., Leurs, R., 2012. Pharmacological modulation of chemokine receptor function. Br. J. Pharmacol. 165, 1617–1643.
Schumacher, T.N., Gerlach, C., van Heijst, J.W., 2010. Mapping the life histories of T cells. Nat. Rev. Immunol. 10, 621–631.
Schwartz, T.W., 1994. Locating ligand-binding sites in 7tm receptors by protein engineering. Curr. Opin. Biotechnol. 5, 434–444.
Shan, L., Qiao, X., Oldham, E., Catron, D., Kaminski, H., Lundell, D., Zlotnik, A., Gustafson, E., Hedrick, J.A., 2000. Identification of viral macrophage inflammatory protein (vMIP)-II as a ligand for GPR5/XCR1. Biochem. Biophys. Res. Commun. 268, 938–941.
Shi, C., Pamer, E.G., 2011. Monocyte recruitment during infection and inflammation. Nat. Rev. Immunol. 11, 762–774.
Slatkin, M., Hudson, R.R., 1991. Pairwise comparisons of mitochondrial DNA sequences in stable and exponentially growing populations. Genetics 129, 555–562.
Springer, T.A., 1995. Traffic signals on endothelium for lymphocyte recirculation and leukocyte emigration. Annu. Rev. Physiol. 57, 827–872.
Sun, J.C., Lanier, L.L., 2011. NK cell development, homeostasis and function: parallels with CD8(+) T cells. Nat. Rev. Immunol. 11, 645–657.
Swanson, W.J., Nielsen, R., Yang, Q., 2003. Pervasive adaptive evolution in mammalian fertilization proteins. Mol. Biol. Evol. 20, 18–20.
Swiecki, M., Colonna, M., 2015. The multifaceted biology of plasmacytoid dendritic cells. Nat. Rev. Immunol. 15, 471–485.
Tajima, F., 1989. Statistical method for testing the neutral mutation hypothesis by DNA polymorphism. Genetics 123, 585–595.
Thompson, J.D., Gibson, T.J., Plewniak, F., Jeanmougin, F., Higgins, D.G., 1997. The CLUSTAL_X windows interface: flexible strategies for multiple sequence alignment aided by quality analysis tools. Nucleic Acids Res. 25, 4876–4882.
Tuinstra, R.L., Peterson, F.C., Kutlesa, S., Elgin, E.S., Kron, M.A., Volkman, B.F., 2008. Interconversion between two unrelated protein folds in the lymphotactin native state. Proc. Natl. Acad. Sci. U.S.A. 105, 5057.
Wang, T., Han, S., Wu, Z., Han, Z., Yan, W., Liu, T., Wei, H., Song, D., Zhou, W., Yang, X., 2015. XCR1 promotes cell growth and migration and is correlated with bone metastasis in non-small cell lung cancer. Biochem. Biophys. Res. Commun. 464, 635.
Watterson, G.A., 1975. On the number of segregating sites in genetical models without recombination. Theor. Popul. Biol. 7, 256–276.
Wise, C.A., Sraml, M., Easteal, S., 1998. Departure from neutrality at the mitochondrial NADH dehydrogenase subunit 2 gene in humans, but not in chimpanzees. Genetics 148, 409.
Wlasiuk, G., Nachman, M.W., 2010. Adaptation and constraint at Toll-like receptors in primates. Mol. Biol. Evol. 27, 2172–2186.
Woo, Y.D., Koh, J., Kang, H.-R., Kim, H.Y., Chung, D.H., 2018. The invariant natural killer T cell–mediated chemokine X-C motif chemokine ligand 1–X-C motif chemokine receptor 1 axis promotes allergic airway hyperresponsiveness by recruiting CD103+ dendritic cells. J. Allergy Clin. Immunol. 142, 1781–1792 e1712.
Yamazaki, C., Miyamoto, R., Hoshino, K., Fukuda, Y., Sasaki, I., Saito, M., Ishiguchi, H., Yano, T., Sugiyama, T., Hemmi, H., Tanaka, T., Hamada, E., Hirashima, T., Amakawa, R., Fukuhara, S., Nomura, S., Ito, T., Kaisho, T., 2010. Conservation of a chemokine system, XCR1 and its ligand, XCL1, between human and mice. Biochem. Biophys. Res. Commun. 397, 756–761.
Yang, Z., 1997. PAML: a program package for phylogenetic analysis by maximum likelihood. Comput. Appl. Biosci. 13, 555–556.
Yang, Z., 2007. PAML 4: phylogenetic analysis by maximum likelihood. Mol. Biol. Evol. 24, 1586–1591.
Yang, Z., Wong, W.S., Nielsen, R., 2005. Bayes empirical bayes inference of amino acid sites under positive selection. Mol. Biol. Evol. 22, 1107–1118.
Yoshida, T., Imai, T., Kakizaki, M., Nishimura, M., Takagi, S., Yoshie, O., 1998. Identification of single C motif-1/lymphotactin receptor XCR1. J. Biol. Chem. 273, 16551–16554.
Yoshida, T., Imai, T., Kakizaki, M., Nishimura, M., Yoshie, O., 1995. Molecular cloning of a novel C or gamma type chemokine, SCM-1. FEBS Lett. 360, 155–159.
Yoshida, T., Izawa, D., T, Nakahara, K., Kakizaki, M., Imai, T., Suzuki, R., Miyasaka, M., Yoshie, O., 1999. Molecular cloning of mXCR1, the murine SCM-1/lymphotactin receptor. FEBS Lett. 458, 37.
Zhang, J., Kumar, S., Nei, M., 1997. Small-sample tests of episodic adaptive evolution: a case study of primate lysozymes. Mol. Biol. Evol. 14, 1335.
Zhang, J., Nielsen, R., Yang, Z., 2005. Evaluation of an improved branch-site likelihood method for detecting positive selection at the molecular level. Mol. Biol. Evol. 22, 2472–2479.
Zlotnik, A., Yoshie, O., 2000. Chemokines: a new classification system and their role in immunity. Immunity 12, 121–127.
Zlotnik, A., Yoshie, O., 2012. The chemokine superfamily revisited. Immunity 36, 705–716.